

Efficacy of perfusion CT in differentiating of pancreatic ductal adenocarcinoma from mass-forming chronic pancreatitis and characterization of isoattenuating pancreatic lesions

Serdar Aslan ¹, Mehmet Selim Nural ², Ilkay Camlidag,² and Murat Danaci²

¹Radiology Clinic, Turhal State Hospital, Turhal, 60300 Tokat, Turkey

²Department of Radiology, Faculty of Medicine, Ondokuz Mayıs University, Samsun, Turkey

Abstract

Purpose: Multidetector computed tomography (MDCT) is routinely used in the diagnosis of pancreatic ductal adenocarcinoma (PDAC), but it may be inadequate in some cases, especially mass-forming chronic pancreatitis (MFCP) and isoattenuating pancreatic lesions. Perfusion CT (pCT) may help resolve this problem. The aim of this study was to evaluate whether pCT could help differentiating PDAC from MFCP and in characterization of isoattenuating pancreatic lesions.

Materials and methods: This prospective study included 89 cases of pancreatic lesions detected by MDCT and further analyzed with pCT. Sixty-one cases with final pathological diagnosis PDAC and 12 cases with MFCP were included from the study. Blood volume (BV), blood flow (BF), mean transit time (MTT), and permeability surface area product (PS) maps were obtained. Perfusion values obtained from the lesions and normal parenchyma were compared.

Results: Compared with normal parenchyma, BV, BF, PS were lower and MTT was longer in PDAC and MFCP ($p < 0.05$). Compared with MFCP, BV, BF, PS were lower and MTT was longer in PDAC ($p < 0.001$). Compared with normal parenchyma, BV, BF, PS were lower and MTT was longer in isoattenuating lesions, ($p < 0.001$). Cutoff values of 7.60 mL/100 mL, 64.43 mL/100 mL/min, 28.08 mL/100 mL/min for BV, BF, PS, respectively, provided 100% sensitivity and specificity and 7.47 s for MTT provided 98.3% sensitivity, 80% specificity for distinguishing PDAC from MFCP.

Conclusion: pCT is a useful technology that can be helpful in overcoming the limitations of routine MDCT in diagnosing PDAC and characterization of isoattenuating lesions.

Key words: Pancreas—Perfusion—Tomography—Adenocarcinoma—Pancreatitis—Chronic

Pancreatic ductal adenocarcinoma (PDAC) continues to be a destructive diagnosis and is expected to become the second leading cause of cancer mortality by 2030 [1]. Due to aggressive course and high mortality, early diagnosis is very important, because it could increase survival by providing a chance for surgical treatment and/or adjuvant intervention [2, 3].

PDAC histologically shows intense fibrosis and, therefore, shows lower contrast enhancement than normal parenchyma in contrast enhanced CT (CECT) [4]. However, PDAC has improved blood flow in 11% to 27%, approximately, and is seen as isoattenuating with parenchyma on CECT [2, 5, 6]. This creates a diagnostic difficulty that may render CECT inadequate for diagnosis.

Another cause of diagnostic difficulty is mass-forming chronic pancreatitis (MFCP). PDAC and MFCP must be differentiated accurately, as their prognosis and management are different. Imaging methods have variable sensitivity and specificity in differentiation of these two pathologies [7]. Morphological evaluation and contrast enhancement properties on routine imaging (CECT and MRI) cannot accurately differentiate PDAC from MFCP, and biopsy is

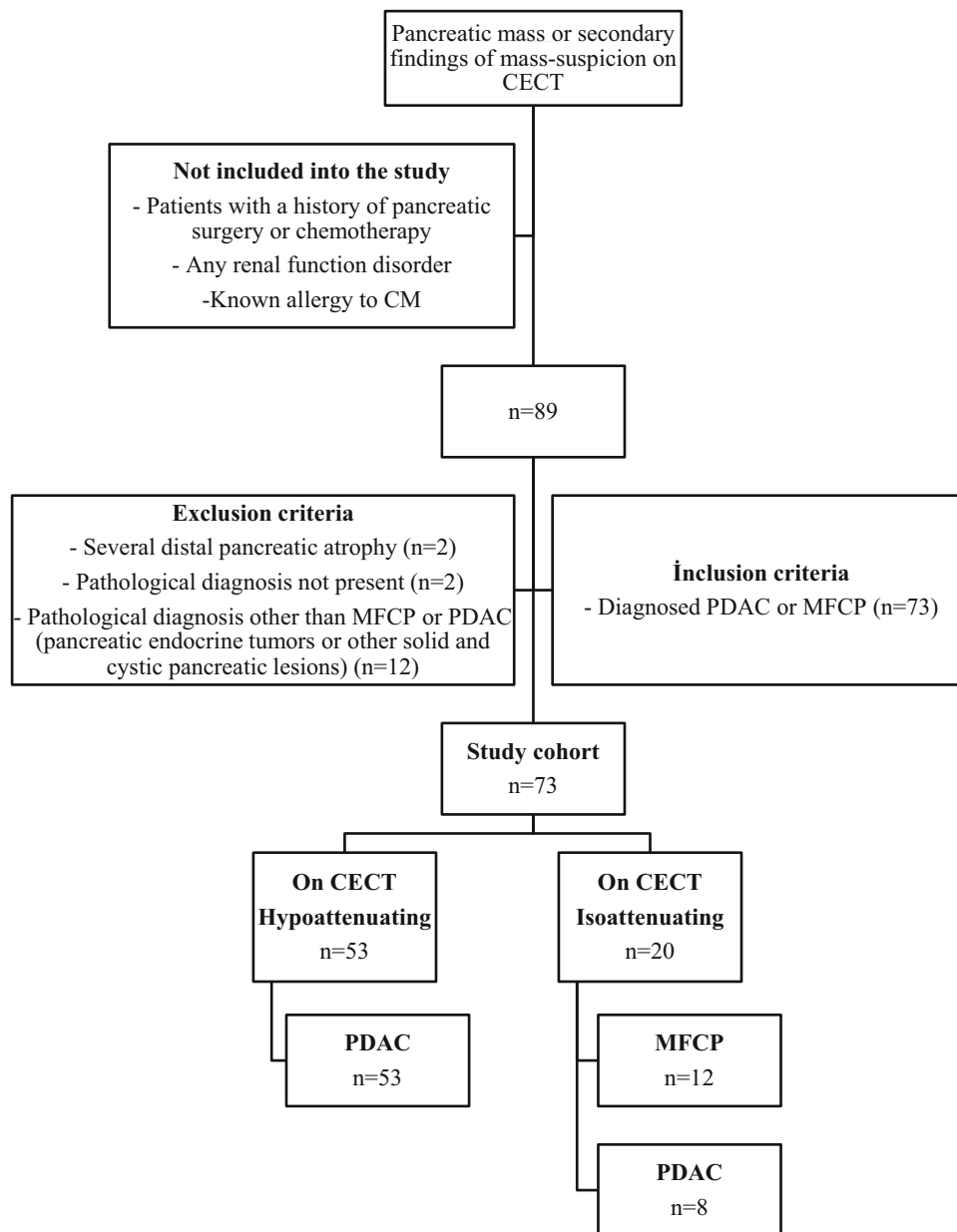


Fig. 1. Flow diagram showing inclusion and exclusion criteria of the study population and CECT imaging features and pathological diagnoses distributions of the cases included in the study.

often needed for diagnosis [8, 9]. However, even EUS-guided biopsies show false negatives at a rate as high as 10%, which is thought to be due to fibrosis around PDAC [7]. Therefore, a more specific imaging method is required to distinguish between these pathologies.

Perfusion CT (pCT) is a non-invasive imaging method based on contrast kinetics of tissue that supplies quantitative information on tissue hemodynamics. In literature, pCT is argued to be a significant method for differentiating benign from malignant lesions, evaluating treatment response, and defining angiogenesis [10–13]. In

a few studies, pCT has been put forth as a promising method for overcoming difficulties encountered in the diagnosis of PDAC [7, 14].

The aim of this study was to assess the utility of pCT in differentiating PDAC from MFCP and in characterizing isoattenuating pancreatic lesions, both of which cause diagnostic difficulty.

Materials and methods

This prospective study was approved by our institutional ethics committee. Informed consent was obtained from all individual participants included in the study.

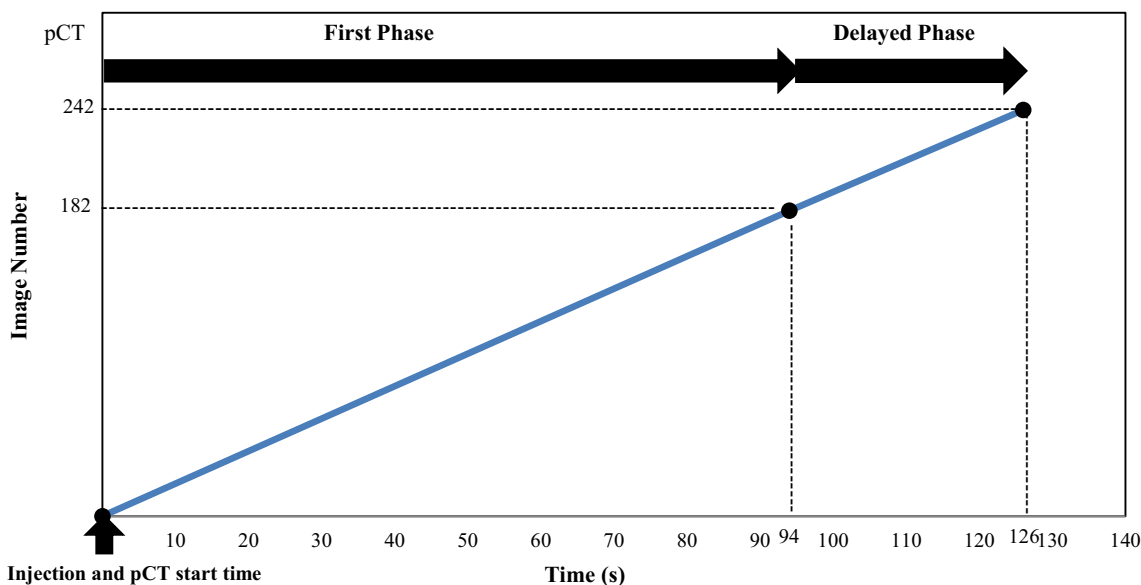


Fig. 2. Time graph of pCT scanning protocol and imaging time points.

Study population

This study was carried out between December 2015 and June 2017. Cases who were scheduled for biphasic pancreatic protocol MDCT examination with a presumed diagnosis of pancreatic tumor were eligible for the study. Pancreatic parenchymal phase images were evaluated on-console by a radiologist for the presence of a tumor or tumor suspicion and the decision to perform pCT was given subsequently. 89 patients with an overt pancreatic tumor or with secondary findings indicative of tumor such as abnormal contour of the pancreas, sudden termination of the choledochal and/or pancreatic duct, and mild to moderate atrophy of the parenchyma distal to the lesion on CECT underwent pCT. Patients with a definite histopathological diagnosis of PDAC or MFCP by either surgery ($n = 44$), percutaneous biopsy ($n = 12$), or endoscopic ultrasound (EUS)-guided fine needle aspiration cytology (FNAC) ($n = 17$) were included in the study. Exclusion criteria were presence of any renal function disorder, a known allergy to contrast medium (CM), history of pancreatic surgery or chemotherapy, absence of a pathological diagnosis or diagnoses other than PDAC or MFCP like endocrine tumors and other cystic and solid masses, and presence of severe distal parenchymal atrophy. The inclusion and exclusion criteria are shown in flow diagram (Fig. 1).

Imaging protocol

MDCT and pCT were performed on 64-slice Dual-Energy CT (Discovery CT750 HD, GE Healthcare, Milwaukee, WI). All cases are laid in supine. Vascular access from antecubital vein was implanted with 18-gauge cannulas. MDCT scanning was performed by with the

help of a power injector (Ulrich Inject CT Motion, Synapse Medical), 80–100 mL of non-ionic CM (Iopamidol:Isovue 370; Bracco, Milan, Italy) with 0.5 g of iodine per kilogram of body weight was administered at a rate of 4 mL/s.

The trigger threshold method was used during the scan to minimize hemodynamic differences. The aortic region of interest (ROI) was placed at the supraceliac level, and the density was measured. Pancreatic parenchymal phase images were taken 20 s after the value of density reached 80 HU. Portal venous phase images were taken after 50 s. Tube voltage 80–140 kVp, tube current 350 mAs, slice thickness 5 mm, field of view (FOV) 300 mm, and rotation time 0.5 s are used during MDCT scanning. All images were obtained as 0.625 mm.

After the on-console evaluation, pCT scanning was performed on cases of mass detection or mass-suspicious secondary findings. In order to cleanse the pancreatic parenchyma of the CM given before the pCT, the patient was immobilized for 15 min on the table. This break was also used to instruct and train patients to breathe slowly and superficially for minimizing breathing artifacts during pCT scanning (shallow breathing). After the break, 50 mL of non-ionic CM was injected using a power injector with a speed of 5 mL/s, and pCT was started simultaneously. 100 kVp of tube voltage, 100 mAs of tube current, a 5 mm slice thickness, a 300 mm FOV, 110 mm z-axis coverage, a pitch of 0.6, a rotation time of 0.28 s, and a cycle time of 0.52 s were used during pCT scanning. We obtained both the first and delayed phases in the pCT scan. The dynamic perfusion scan was equally distributed along the timeline. The total number of images obtained in pCT was 242 (first phase 182, delayed phase 60), and scanning time was 126 s (first phase 94 s,

Table 1. Results of perfusion parameters of lesions and normal parenchyma measured by both readers in PDAC cases

Parameter	PDAC	Normal parenchyma of PDAC	<i>p</i>
BV (mL/100 mL)			
Reader 1	2.80 ± 1.14	17.64 ± 4.25	< 0.001
Reader 2	2.76 ± 1.24	18.60 ± 4.95	< 0.001
BF (mL/100 mL/min)			
Reader 1	31.55 ± 11.54	118.61 ± 36.42	< 0.001
Reader 2	30.36 ± 10.86	121.88 ± 36.11	< 0.001
MTT (s)			
Reader 1	11.26 ± 2.94	3.68 ± 0.88	< 0.001
Reader 2	11.39 ± 2.90	3.57 ± 0.89	< 0.001
PS (mL/100 mL/min)			
Reader 1	12.83 ± 3.99	52.83 ± 5.92	< 0.001
Reader 2	11.88 ± 4.52	53.91 ± 6.78	< 0.001

Results were expressed in mean ± [SD]. Statistical significance level was set as $p < 0.05$. The significant p values have been highlighted in bold

delayed phase 32 s). The time graph of pCT scanning protocol and imaging time points are shown in Fig. 2.

Total dose length product (DLP) for the pCT examination was recorded for each patient. The formula $DLP \times$ conversion factor (0.015) was used for effective dose calculation.

Image analysis

All analyses were independently performed by two different radiologists with different levels of experience (a board-certified radiologist with 5 and 12 years of experience in abdominal radiology) who were blinded to each other and histopathological results. The hypoattenuating and isoattenuating mass/mass-suspicious areas were deemed as lesions on CECT and analyzed on pCT. In addition, isoattenuating masses were defined as those with a 10–15-HU attenuation difference compared with adjacent parenchyma. If no mass were visible, the radiologists were instructed to place the “isoattenuating masses” ROI at the site of the abrupt main pancreatic duct termination or any focal irregularity in the contour of the pancreas. Raw data images of pCT scanning were evaluated at a perfusion software-equipped workstation (AW Server; GE Medical Systems). The software used the deconvolution model. A reference arterial input curve was obtained by placing an ROI in the aorta, followed by blood vessel segmentation and calculation of perfusion maps. Perfusion parameters like blood flow (BF), blood volume (BV), mean transit time (MTT), and permeability surface area product (PS) were analyzed on these maps. The area of ROIs was standardized for both radiologists at 15 mm² using the computer. Then, ROIs were placed to the mass/mass-suspicious area and to normal parenchyma. In all cases, normal parenchyma ROI was placed to the farthest area from the lesion. Placing ROIs, vascular structures, and pancreatic ducts were avoided and solid areas of lesions were measured.

Statistical analysis

Statistical analyses were done with SPSS software, version 21 (IBM Corporation, Armonk, NY, USA). All parameter were expressed as mean ± [SD]. Perfusion values measured from lesions in each case, which were segregated according to pathological diagnosis, were compared with those of normal parenchyma from the same respective case. Perfusion values measured from lesions in cases of PDAC were compared with cases of MFCP. Cases of isoattenuating lesions on CECT were categorized as a subgroup, and the perfusion values measured were compared with those of normal parenchyma. Then, cases of isoattenuating lesions were segregated according to pathological diagnosis, and perfusion values for cases of PDAC were compared with those of MFCP.

The Shapiro–Wilk test was used to test the normality of the data. In dependent measures, a paired samples t-test was used for variables that showed normal distribution, and the Wilcoxon signed-rank test was used for variables that did not show normal distribution. In independent measures, an independent samples t-test was used for variables that showed normal distribution and the Mann–Whitney U test was used for variables that did not show normal distribution. ROC analysis was used for perfusion parameters in order to specify the cutoff for differentiation of MFCP from PDAC.

To assess intrareader agreement and evaluate the reliability of the measurements, interclass correlation coefficients (ICCs) were used. ICCs greater than 0.90 were classified as high, ICCs between 0.70–0.89 as substantial, and ICCs less than 0.70 as in poor agreement.

Results

Seventy-three cases (34 woman–39 men; mean age 68 ± 0.8 years; range, 27–90) were finally included in the study. Sixty-one cases received a pathological diagnosis of PDAC (12 on percutaneous biopsy, 17 on EUS-guided FNAC, and 44 via surgery). Of 12 MFCP cases, 8 were

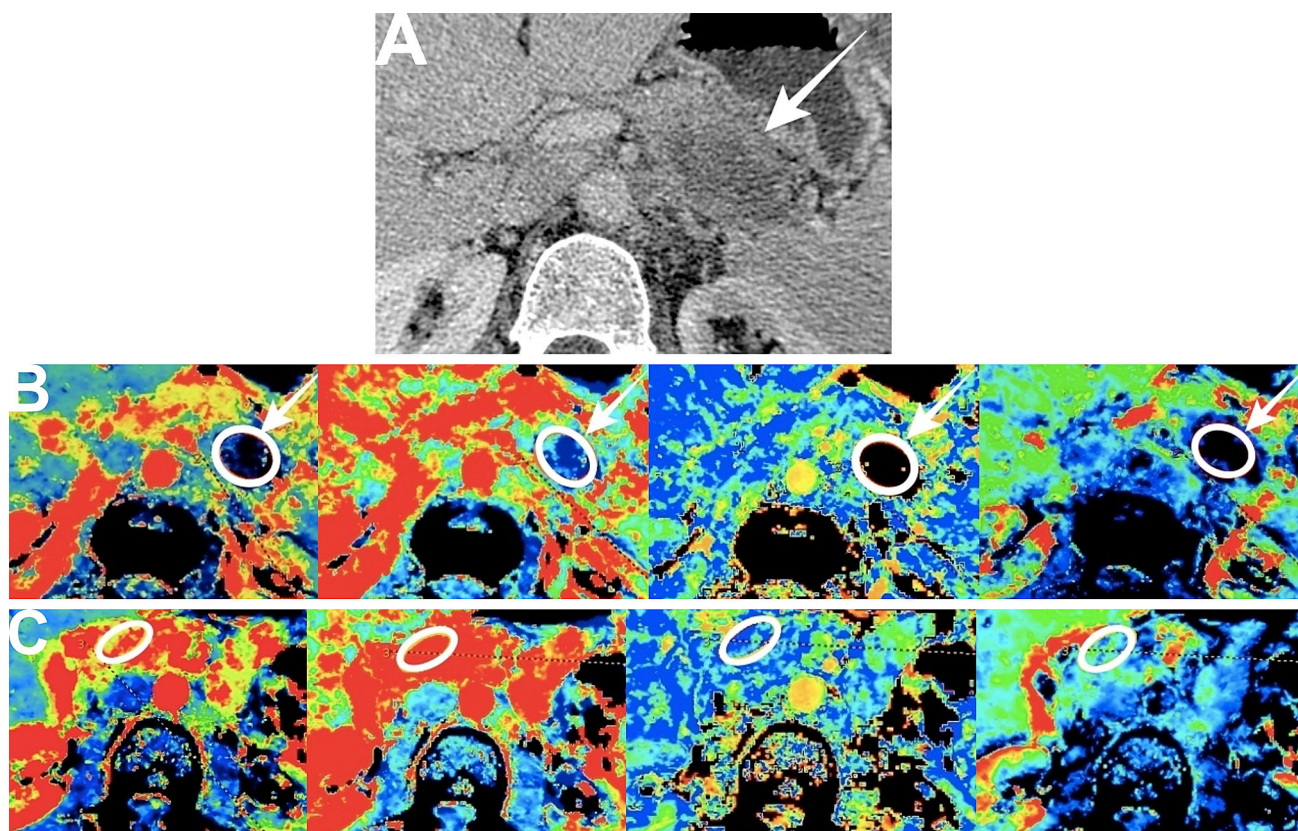


Fig. 3. A 65-year-old female patient whose PDAC was pathologically confirmed. **(A)** Hypoattenuating tumor located in pancreatic tail is seen on CECT (arrow). **(B, C)** On BV, BF, MTT, and PS maps, lesions (arrows, circle) with lower

perfusion and prolonged transit times compared to normal parenchyma (circle) can be monitored visually and by the results of the measurements.

Table 2. Results of perfusion parameters of lesions and normal parenchyma measured by both readers in MFCP cases

Parameter	MFCP	Normal parenchyma of MFCP	<i>p</i>
BV (mL/100 mL)			
Reader 1	11.24 ± 0.81	19.37 ± 4.01	< 0.014
Reader 2	10.70 ± 0.84	19.34 ± 4.01	< 0.008
BF (mL/100 mL/min)			
Reader 1	79.73 ± 3.03	130.12 ± 18.21	< 0.001
Reader 2	80.53 ± 4.84	131.32 ± 16.53	< 0.001
MTT (s)			
Reader 1	7.03 ± 1.47	3.81 ± 0.99	< 0.001
Reader 2	7.20 ± 1.17	4.11 ± 0.72	< 0.001
PS (mL/100 mL/min)			
Reader 1	37.02 ± 3.34	54.91 ± 0.54	< 0.001
Reader 2	36.60 ± 2.71	54.06 ± 1.14	< 0.001

Results were expressed in mean ± [SD]. Statistical significance level was set as $p < 0.05$. The significant p values have been highlighted in bold

diagnosed by EUS-guided FNAC and 4 were diagnosed by percutaneous biopsy. MFCP cases have been followed for 15–24 months, and none has been developed malignancy. A flow diagram on pathological diagnosis distribution and MDCT scanning features in cases where pCT was performed is presented in Fig. 1.

Of the PDAC cases, 34 were male and 27 were female (age 68.9 ± 9.9 years, range 45–90 years). 42 lesions

were located in the head of the pancreas, 16 in the body, and 3 in the tail, with a mean size of 34.2 ± 15.6 mm (range 13–94 mm). Of the MFCP cases, 5 were male and 7 were female (age 55.6 ± 16.5 years, range 27–70 years). Eight lesions were located in the head of the pancreas and 4 in the body, with a mean size of 16.3 ± 4.0 mm (range 15–21 mm).

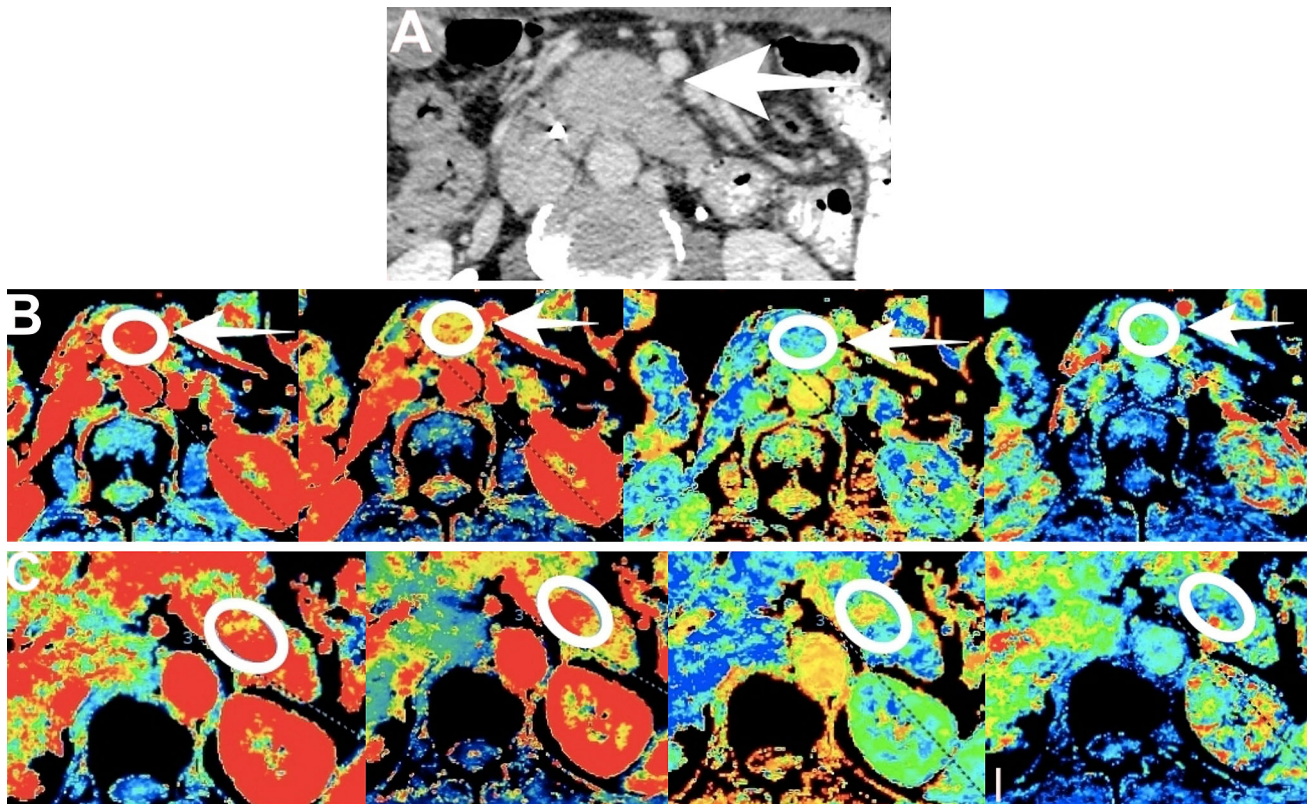


Fig. 4. A 51-year-old male patient whose MFCP was pathologically confirmed. In the case, malignancy did not develop during the 18-month follow-up period. **(A)** An isoattenuating mass view with parenchyma in the body of pancreas is monitored on CECT (arrow). **(B, C)** On BV, BF,

MTT, and PS maps, lesions (arrows, circle) demonstrated low perfusion and prolonged transit times compared to normal parenchyma (circle) can be monitored both visually and by the results of the measurements.

Significant differences in perfusion parameters were noted between tumors and normal parenchyma in PDAC cases ($p < 0.001$), as shown in Table 1 (Fig. 3A–C). Perfusion values for tumors in PDAC cases were found to be lower than those for normal parenchyma by 84.2%–85.2% for BV, 73.5%–75.1% for BF, and 75.8%–78.0% for PS, while MTT was 67.4%–68.7% longer (readers 1 and 2, respectively).

Significant differences in perfusion parameters were noted between lesions and normal parenchyma in MFCP cases ($p < 0.05$), as shown in Table 2 (Fig. 4A–C). Perfusion values for lesions in MFCP cases were found to be lower than those for normal parenchyma by 41.9%–44.6% for BV, 38.7%–38.6% for BF, and 33.4%–31.7% for PS, while MTT was 45.8%–42.9% longer (readers 1 and 2, respectively).

For PDAC and MFCP cases, distribution of perfusion parameters for readers was presented in box-plot graphics (Fig. 5).

Significant differences in perfusion parameters were noted between cases of PDAC and MFCP ($p < 0.001$). Perfusion values for lesions in PDAC cases were found to be lower than those for MFCP cases by 76.3%–75.4% for BV, 60.2%–62.1% for BF, and 65.1%–68% in PS, while

MTT was 36.5%–36.2% longer (readers 1 and 2, respectively). There were no significant differences between perfusion values measured from normal parenchyma in each group (Table 3).

When 20 cases of isoattenuating lesions were measured against normal parenchyma from the same respective cases, BV, BF, and PS were lower, and MTT was longer ($p < 0.001$) (Table 4). Perfusion values for isoattenuating lesions were found to be lower than those of normal parenchyma by 65.9%–68.3% for BV, 55.9%–56.5% for BF, and 57.7%–59.2% for PS, while MTT was 58.4%–60.2% longer (readers 1 and 2, respectively). When isoattenuating lesions from cases of PDAC diagnosis were measured against isoattenuating lesions from cases of MFCP diagnosis, BV, BF, and PS were lower, and MTT was longer ($p < 0.05$) (Table 4). Perfusion values in cases of PDAC diagnosis were found to be lower than those in cases of MFCP diagnosis by 74.3%–73.5% for BV, 52.1%–56.1% for BF, and 64.5%–66.2% for PS, while MTT was 38.4%–37.1% longer (readers 1 and 2, respectively).

Intrareader agreements for pCT parameters are shown in Table 5. As there was higher intrareader agreement in PDAC and MFCP cases, average perfusion

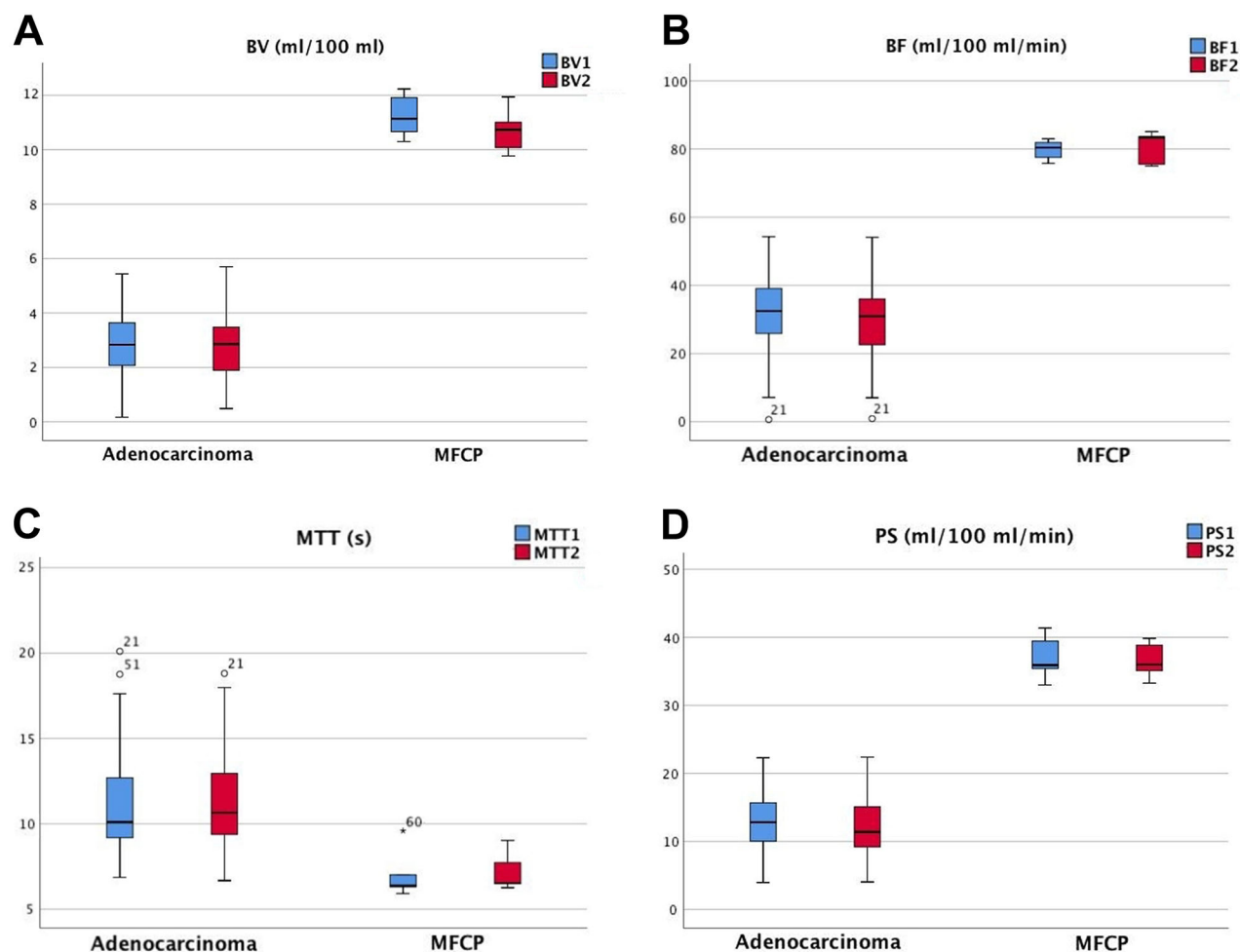


Fig. 5. Distribution of BV (A), BF (B), MTT (C), and PS (D) parameters is monitored for each reader (blue color; reader 1, red color; reader 2) in the box-plot charts according

values were calculated for all parameters, and optimal cutoff values were determined by ROC analysis. When BV, BF, PS, and MTT were chosen as 7.60 mL/100 mL, 64.43 mL/100 mL/min, 28.08 mL/100 mL/min, and 7.47 s, respectively, differentiation between PDAC and MFCP was accomplished with high sensitivity (100%, 100%, 100%, and 98.3%, respectively) and specificity (100%, 100%, 100%, and 80%, respectively) (Fig. 6).

In our study, the DLP (mean \pm SD) for the entire pCT examination was 480 ± 125 mGy.cm, using CTDIvol mean 6.7 mGy. The average radiation dose of the pCT examination was 6.3 ± 2.1 mSv.

Discussion

Our study indicated that BV, BF, and PS were significantly lower and MTT was significantly longer in PDAC compared to normal parenchyma. Yadav et al. reported that BV, BF, and PS values for lesions were significantly lower and MTT significantly longer than those for normal parenchyma in a study of 42 PDAC cases [7]. Similar

to pathological diagnoses, respectively. The mean values of BV, BF, PS for both readers were lower in PDAC cases than in MFCP, and MTT was longer.

results were reported by Xu et al. [15], Delrue et al. [16], and Klaus et al. [17]. Our findings are consistent with those of previous studies.

BF is regarded as the most important parameter relating to tissue perfusion [15]. The fibrosis seen in PDAC and the associated intratumoral pressure increase are thought to result in lower BF and BV [4]. As to the PS, indicates capillary membrane permeability and also expected to be lower in PDAC due to intratumoral blood vessel infiltration and fibrosis. Moreover, the decrease in BF and BV in PDAC indirectly decreases PS [18, 19]. Delayed phase scanning (> 40 s) is required to obtain the PS measurement correctly. Obtaining the delayed phase scanning allows the capillary permeability to be accurately determined by detecting contrast extravasation in the intravascular compartment along the capillary walls of the extravascular compartment. Our study along with many other studies in the literature yielded lower PS values in PDAC [7, 15–17]. However, Zhao et al. found higher PS values in PDAC. We think that this contra-

Table 3. Results of perfusion parameters of lesions and normal parenchyma measured by both readers PDAC and MFCP cases

Parameter	PDAC	MFCP	Normal parenchyma of PDAC	Normal parenchyma of MFCP	<i>p</i>
BV (mL/100 mL)					
Reader 1	2.80 ± 1.14	11.24 ± 0.81	17.64 ± 4.25	19.37 ± 4.01	< 0.001 to 0.419
Reader 2	2.76 ± 1.24	10.70 ± 0.84	18.60 ± 4.95	19.34 ± 4.01	< 0.001 to 0.748
BF (mL/100 mL/min)					
Reader 1	31.55 ± 11.54	79.73 ± 3.03	118.61 ± 36.42	130.12 ± 18.21	< 0.001 to 0.238
Reader 2	30.36 ± 10.86	80.53 ± 4.84	121.88 ± 36.11	131.32 ± 16.53	< 0.001 to 0.288
MTT (s)					
Reader 1	11.26 ± 2.94	7.03 ± 1.47	3.68 ± 0.88	3.81 ± 0.99	< 0.001 to 0.574
Reader 2	11.39 ± 2.90	7.20 ± 1.17	3.57 ± 0.89	4.11 ± 0.72	< 0.001 to 0.161
PS (mL/100 mL/min)					
Reader 1	12.83 ± 3.99	37.02 ± 3.34	52.83 ± 5.92	54.91 ± 0.54	< 0.001 to 0.288
Reader 2	11.88 ± 4.52	36.60 ± 2.71	53.91 ± 6.78	54.06 ± 1.14	< 0.001 to 0.793

Results were expressed in mean ± [SD]. *p* < 0.05 (Adenocarcinoma—MFCP, Normal parenchyma of adenocarcinoma—Normal parenchyma of MFCP, respectively) was taken as statistically significant. The significant *p* values have been highlighted in bold

Table 4. Results of perfusion parameters in lesions and normal parenchyma measured by both readers in cases with isoattenuating lesions

Parameter	Isoattenuating lesion	Normal parenchyma of isoattenuating lesion	Isoattenuating PDAC	Isoattenuating MFCP	<i>p</i>
BV (mL/100 mL)					
Reader 1	6.37 ± 4.35	18.63 ± 3.30	2.89 ± 0.66	11.24 ± 0.81	< 0.001 to < 0.001
Reader 2	6.11 ± 4.11	19.25 ± 4.46	2.84 ± 0.71	10.70 ± 0.84	< 0.001 to < 0.001
BF (mL/100 mL/min)					
Reader 1	55.51 ± 21.95	125.86 ± 28.10	38.21 ± 6.30	79.74 ± 3.00	< 0.001 to < 0.001
Reader 2	54.20 ± 23.86	124.47 ± 24.92	35.39 ± 6.18	80.53 ± 4.84	< 0.001 to < 0.001
MTT (s)					
Reader 1	9.58 ± 2.85	3.99 ± 1.11	11.40 ± 2.05	7.03 ± 1.47	< 0.001 to 0.002
Reader 2	9.67 ± 3.03	3.79 ± 1.02	11.44 ± 2.68	7.20 ± 1.17	< 0.001 to 0.005
PS (mL/100 mL/min)					
Reader 1	23.10 ± 13.04	54.56 ± 3.13	13.16 ± 5.25	37.02 ± 3.34	< 0.001 to < 0.001
Reader 2	22.47 ± 13.26	55.02 ± 4.70	12.38 ± 5.71	36.60 ± 2.71	< 0.001 to < 0.001

Results were expressed in mean ± [SD]. *p* < 0.05 (Isoattenuating lesion—Normal parenchyma, Isoattenuating PDAC—Isoattenuating MFCP, respectively) was taken as statistically significant. The significant *p* values have been highlighted in bold

dictory result could be explained by the fact that their measurements were obtained from the first phase scans and they did not perform delayed phase scanning which is (> 40 s) required for correct measurement of PS [20]. We also performed delayed phase scanning in order to evaluate transmittance more accurately as the other studies that had similar results to ours with regard to PS.

The number of studies evaluating the MTT parameter is limited. Yadav et al. demonstrated that MTT was longer in PDAC than normal parenchyma; however, Xu et al. stated that MTT in PDAC did not differ from that of normal parenchyma [7, 15]. Considering the histological characteristics of PDAC, prolongation of MTT is expected. We think that the variability in results is due to the use of different scanners, protocols, and mathematical methods; however, the fact that both readers in our study obtained similar results suggests that our results are not derived from differences in personal experience [20, 21]. Further studies will be necessary to gather reliable information on this issue.

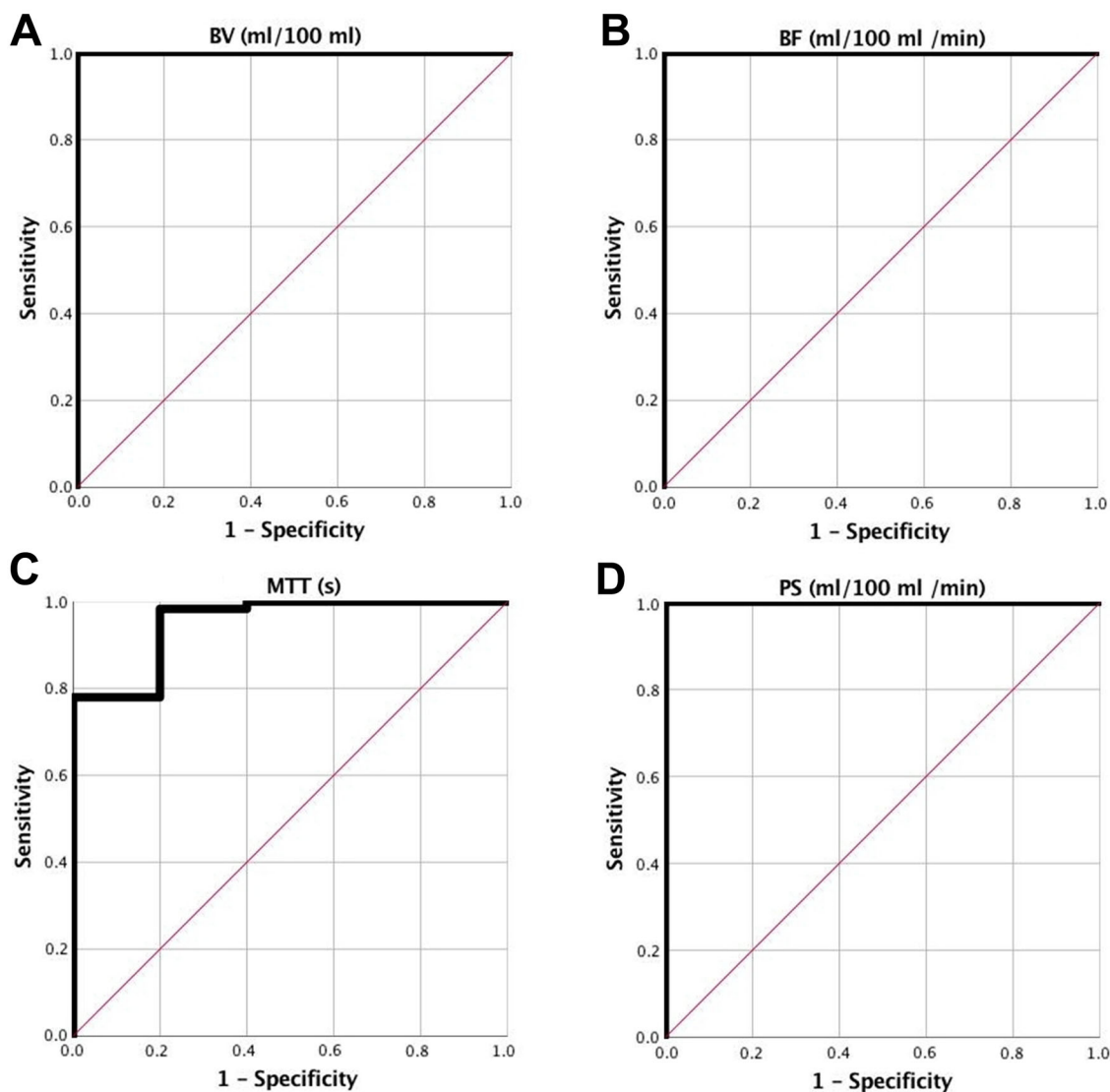
In our study, we found that BV, BF, and PS values were significantly lower and MTT was significantly longer in masses in MFCP cases compared to normal

parenchyma. Fibrosis-associated endothelial damage seen in MFCP is responsible for the decrease in BF and PS, and degradation of vascular structures for the decrease in BV. It is expected that MTT is also prolonged with the decrease in microvascular structure density. Yadav et al. indicated in their study with 13 MFCP cases that BV, BF, and PS values measured from masses were significantly lower than those of normal parenchyma, but that MTT was not statistically significant [7]. Our findings on BV, BF and PS are consistent with that study.

The most important cause of difficulty in diagnosis of PDAC is MFCP. When we compared perfusion parameters for 61 PDAC and 12 MFCP cases, we found significantly lower BV, BF, and PS and MTT significantly longer in PDAC cases compared to MFCP cases. In other studies in the literature, Yadav et al. also reported BV as lower by 43.6%, BF by 45.3%, and PS by 35.3% in PDAC compared to MFCP, and Lu et al. reported BF as lower by 56% and BV by 53% [7, 14]. We think that these differences are not surprising because the density of microvascular structures in PDAC is less than that of MFCP, a hypothesis supported by the observation of lower BV and BF values in PDAC. Similarly, intratu-

Table 5. Intrareader agreement for perfusion parameters between readers according to histopathological diagnoses

Perfusion parameters	Mean ICCs (%95 CI) between readers		
	Adenocarcinoma	MFCP	Isoattenuating lesions
BV	0.94 (0.90–0.97)	0.96 (0.93–0.98)	0.90 (0.80–0.95)
BF	0.95 (0.69–0.99)	0.98 (0.83–0.99)	0.76 (– 0.11–0.97)
MTT	0.88 (– 0.12–0.98)	0.96 (0.71–0.99)	0.89 (– 0.06–0.98)
PS	0.99 (0.98–0.99)	0.96 (0.86–0.99)	0.99 (0.97–0.99)

**Fig. 6.** ROC curve and AUC analysis for BV (A), BF (B), MTT (C), PS (D) for differentiating between PDAC and MFCP. AUC, sensitivity, and specificity for all parameters were quite high.

moral blood vessel infiltration and fibrosis in PDAC is more pronounced than in MFCP, and this situation explains the difference in PS value. Our results for PDAC–MFCP differentiation were in line with the previous studies. However, our results have a higher diagnostic accuracy than the results of Yadav et al., which used a similar pCT method [7]. We think that this situation is

due to the high number of PDAC cases in our study. Also, in our study, the perfusion values of the lesions were obtained by placing the ROI of the solid areas of the lesions. In our study, higher number of PDAC cases and almost the same number of MFCP cases according to other study, and also obtained perfusion values from measurements of the solid areas of the lesions may be

explain the higher diagnostic accuracy we find. However, the use of different scanners and mathematical methods, despite the use of the same pCT method, may have led to a higher diagnostic accuracy in our study.

In the literature, there were many reports showing that FDG-PET/CT is a sensitive and specific non-invasive technique and is therefore useful in differentiating pancreatic cancer from mass-forming chronic pancreatitis [22–24]. However, it was shown that there were certain limitations to FDG-PET/CT in the diagnosis of pancreatic cancer and that false-negative cases might occur when the tumor was less than 1 cm in diameter [25]. Also, Kato et al. reported that it is difficult to differentiate between metastasis-free pancreatic cancer and mass-forming pancreatitis by FDG-PET/CT due to a considerable overlap between the SUVmax values of the two diseases [26]. On the other hand, because FDG is not a tumor-specific substance, inflammatory pancreatic diseases could give rise to focal FDG uptake in the same intensity range as pancreatic cancer [27]. These findings may result in low specificity of FDG-PET/CT in differentiating malignant tumors from benign lesions. Thus, obscure points still remain about the usefulness of FDG-PET/CT in differentiating pancreatic cancer from chronic pancreatitis.

Isoattenuating pancreatic lesions are another diagnostic challenge. Prokesch et al. reported that evaluation based on density in isoattenuating lesions might be insufficient [5]. Yadav et al. reported that 6 of 42 PDAC cases were isoattenuating in MDCT and could be distinguished on perfusion maps [7]. In our study, we could also distinguish isoattenuating lesions from normal parenchyma by both visual identification on perfusion maps and comparison of perfusion values.

The greatest barrier to the routine use of pCT is the high radiation dose required. In our study, as MDCT scans were performed prior to pCT, unenhanced scans were not performed. For pCT, the lowest value allowed by the z-axis coverage scanner was selected. An adaptive iterative reconstruction algorithm was used to reduce the radiation dose. Radiation doses in pCT studies in the literature are reported by Yadav et al. as 12.6 ± 1.34 mSv, and by Kandel et al. as 10.1 mSv [7, 12]. The dose in our study was at the acceptable level when compared to other studies.

Our study has some limitation. Firstly, the number of MFPC cases evaluated in this study was low. MFPC is a relatively rare entity, and limitations associated with a small number of cases are also present in the literature. The results reported in this study need to be tested in a larger cohort of patients. Secondly, we compared perfusion values measured from lesions in PDAC and MFPC cases with normal parenchyma in the same respective cases. This study did not employ a control group. It is indicated in the literature that perfusion values between normal parenchyma in healthy cases and

normal parenchyma in PDAC cases are the same [15, 17] and this does not constitute a handicap.

In conclusion, our study has shown that pCT is a useful technique for characterizing lesions and for overcoming difficulties encountered in the assessment of density measurement and morphology in PDAC diagnosis. We have shown that pCT can be used for and may additionally contribute to research on the differentiation of MFPC from PDAC, which is a cause of difficulty in diagnosis, and that pCT is also effective in the detection of isoattenuating lesions.

Compliance with ethical standards

Funding No funding was received for this study.

Conflict of interest The authors declare that they have no conflict of interest.

Ethical approval All procedures performed in studies involving human participants were in accordance with the ethical standards of the institutional research committee and the 1964 Declaration of Helsinki and its later amendments or comparable ethical standards. For this type of study formal consent is not required.

References

1. Rahib L, Smith BD, Aizenberg R, et al. (2014) Projecting cancer incidence and deaths to 2030: the unexpected burden of thyroid, liver, and pancreas cancers in the United States. *Cancer Res* 74:2913–2921
2. Klauss M, Stiller W, Pahn G, et al. (2013) Dual-energy perfusion-CT of pancreatic adenocarcinoma. *Eur J Radiol* 82:208–214
3. Kim R, Saif MW (2007) Is there an optimal neoadjuvant therapy for locally advanced pancreatic cancer? *JOP* 8:279–288
4. Grözinger G, Grözinger A, Horger M (2014) The role of volume perfusion CT in the diagnosis of pathologies of the pancreas. *Fortschr Röntgenstr* 186:1082–1093
5. Prokesch RW, Chow LC, Beaulieu CF, Bammer R, Jeffrey RB (2002) Isoattenuating pancreatic adenocarcinoma at multi-detector row CT: secondary signs. *Radiology* 224:764–768
6. Kim JH, Park SH, Yu ES, et al. (2010) Visually isoattenuating pancreatic adenocarcinoma at dynamic-enhanced CT: frequency, clinical and pathologic characteristics, and diagnosis at imaging examinations. *Radiology* 257:87–96
7. Yadav AK, Sharma R, Kandasamy D, et al. (2016) Perfusion CT—can it resolve the pancreatic carcinoma versus mass forming chronic pancreatitis conundrum? *Pancreatol* 16:979–987
8. Sahani DV, Kalva SP, Farrell J, et al. (2004) Autoimmune pancreatitis: imaging features. *Radiology* 233:345–352
9. Chang WI, Kim BJ, Lee JK, et al. (2009) The clinical and radiological characteristics of focal mass-forming autoimmune pancreatitis: comparison with chronic pancreatitis and pancreatic cancer. *Pancreas* 38:401–408
10. Ichikawa T, Sou H, Araki T, et al. (2001) Duct-penetrating sign at MRCP: usefulness for differentiating inflammatory pancreatic mass from pancreatic carcinomas. *Radiology* 221:107–116
11. Hartwig W, Schneider L, Diener MK, et al. (2009) Preoperative tissue diagnosis for tumours of the pancreas. *Br J Surg* 96:5–20
12. Kandel S, Kloeters C, Meyer H, et al. (2009) Whole-organ perfusion of the pancreas using dynamic volume CT in patients with primary pancreas carcinoma: acquisition technique, post-processing and initial results. *Eur Radiol* 19:2641–2646
13. Miles KA, Charnsangavej C, Lee FT, et al. (2000) Application of CT in the investigation of angiogenesis in oncology. *Acad Radiol* 7:840–850
14. Lu N, Feng XY, Hao SJ, et al. (2011) 64-slice CT perfusion imaging of pancreatic adenocarcinoma and mass-forming chronic pancreatitis. *Acad Radiol* 18:81–88

15. Xu J, Liang Z, Hao S, et al. (2009) Pancreatic adenocarcinoma: dynamic 64-slice helical CT with perfusion imaging. *Abdom Imaging* 34:759–766
16. Delrue L, Blanckaert P, Mertens D, et al. (2011) Assessment of tumor vascularization in pancreatic adenocarcinoma using 128-slice perfusion computed tomography imaging. *J Comput Assist Tomogr* 35:434–438
17. Klauss M, Stiller W, Fritz F, et al. (2012) Computed tomography perfusion analysis of pancreatic carcinoma. *J Comput Assist Tomogr* 36:237–242
18. Bluemke DA, Cameron JL, Hruban RH, et al. (1995) Potentially resectable pancreatic adenocarcinoma: spiral CT assessment with surgical and pathologic correlation. *Radiology* 197:381–385
19. Eastwood JD, Lev MH, Provenzale JM (2003) Perfusion CT with iodinated contrast material. *AJR* 180:3–12
20. Zhao X, Zhou C, Wu N, et al. (2003) Study of multiple slices pancreatic CT perfusion. *Chin J Radiol* 37:845–849
21. Kudo K, Sasaki M, Yamada K, et al. (2009) Differences in CT perfusion maps generated by different commercial software: quantitative analysis by using identical source data of acute stroke patients. *Radiology* 254:200–209
22. van Kouwen MC, Jansen JB, van Goor H, et al. (2005) FDG-PET is able to detect pancreatic carcinoma in chronic pancreatitis. *Eur J Nucl Med Mol Imaging* 32:399–404
23. Keogan MT, Tyler D, Clark L, et al. (1998) Diagnosis of pancreatic carcinoma: role of FDG PET. *AJR* 171:1565–1570
24. Ruan Z, Jiao J, Min D, et al. (2018) Multimodality imaging features distinguish pancreatic carcinoma from mass-forming chronic pancreatitis of the pancreatic head. *Oncol Lett* 15:9735–9744
25. Delbeke D, Pinson CW (2004) Pancreatic tumors: role of imaging in the diagnosis, staging, and treatment. *J Hepatobil Pancreat Surg* 11:4–10
26. Kato K, Nihashi T, Ikeda M, et al. (2013) Limited efficacy of ¹⁸F-FDG PET/CT for differentiation between metastasis-free pancreatic cancer and mass-forming chronic pancreatitis. *Clin Nucl Med* 38:417–421
27. Ozaki Y, Oguchi K, Hamano H, et al. (2008) Differentiation of autoimmune pancreatitis from suspected pancreatic cancer by fluorine-18 fluorodeoxyglucose positron emission tomography. *J Gastroenterol* 43:144–151